

Online Research @ Cardiff

This is an Open Access document downloaded from ORCA, Cardiff University's institutional repository: <https://orca.cardiff.ac.uk/id/eprint/138143/>

This is the author's version of a work that was submitted to / accepted for publication.

Citation for final published version:

Almudaihesh, F., Alfaris, H., Sangha, P., Pullin, R. ORCID:
<https://orcid.org/0000-0002-2853-6099> and Eaton, M. ORCID:
<https://orcid.org/0000-0002-7388-6522> 2021. Understanding the role of
graphene on the moisture absorption in graphene/polymer nanocomposites.
IOP Conference Series: Materials Science and Engineering 1024 (1) , 012006.
10.1088/1757-899X/1024/1/012006 file

Publishers page: <http://dx.doi.org/10.1088/1757-899X/1024/1/012006>
<<http://dx.doi.org/10.1088/1757-899X/1024/1/012006>>

Please note:

Changes made as a result of publishing processes such as copy-editing, formatting and page numbers may not be reflected in this version. For the definitive version of this publication, please refer to the published source. You are advised to consult the publisher's version if you wish to cite this paper.

This version is being made available in accordance with publisher policies.

See

<http://orca.cf.ac.uk/policies.html> for usage policies. Copyright and moral rights for publications made available in ORCA are retained by the copyright holders.



PAPER • OPEN ACCESS

Understanding the Role of Graphene on the Moisture Absorption in Graphene/Polymer Nanocomposites

To cite this article: F Almudaihesh *et al* 2021 *IOP Conf. Ser.: Mater. Sci. Eng.* **1024** 012006

View the [article online](#) for updates and enhancements.

Understanding the Role of Graphene on the Moisture Absorption in Graphene/Polymer Nanocomposites

F Almudaihesh¹, H Alfaris¹, P Sangha¹, R Pullin¹, M Eaton¹

¹ Cardiff School of Engineering, Cardiff University, Cardiff, UK

Email: almudaiheshfs@cardiff.ac.uk

Abstract. This study focuses on understanding the effect of graphene, when introduced in epoxy systems, on the overall moisture absorption capacity and behaviour of epoxy resin composites subjected to hydrothermal conditions. Pristine epoxy resin and epoxy resin incorporating functionalised and unfunctionalised graphene reinforcement were manufactured and exposed to 90°C purified water for 30 days. The flexural and tensile properties were observed for both unaged and aged specimens. A lower moisture absorption capacity was observed for graphene enhanced specimens as opposed to pristine epoxy resin, which suggests the potential of graphene as a barrier to moisture ingress. Despite the lower mass gain observed, the performance of the nano-filled resins exhibits a larger reduction in properties following water absorption.

1. Introduction

Advanced fibrous/polymeric composite materials are attractive for use in the aviation industry, due to their excellent strength and stiffness-to-weight ratios as well as their improved corrosion resistance. However, aerospace materials are exposed to extreme environments and must sustain moisture absorption, pressure variation and impact. It is therefore essential to understand the behaviour of epoxy composites under such harsh conditions. Many studies have been carried out to understand the role of moisture absorption on the performance of fibrous composites [1–4]. More recently, nanocomposites have attracted interest from the aerospace sector for their potential to enhance mechanical properties and further reduce weight. Relevant examples include the Airbus A350 horizontal tail leading edge [5], in which graphene was incorporated within the resin of the structural material.

Generally, polymers in polymeric composites are degradable when in contact with moist environments where chain scission promotes thermophysical and mechanical changes through hydrolysis in which water molecules interrupt the inter-chain hydrogen bonds [6] leading to essential changes in the overall intrinsic structural performance [7]. The interfacial regions are of particular concern where water molecules penetrate through micro-cracks into the structure and settle in the interfacial regions between the matrix and the reinforcements leading to further matrix degradation and interfacial debonding [8,9], as illustrated in Figure 1 [10].

This study is to better understand the effect of graphene when introduced into epoxy systems and how they behave under moist environments prior to adding them in other forms of structural composites such as polymer/carbon composites.



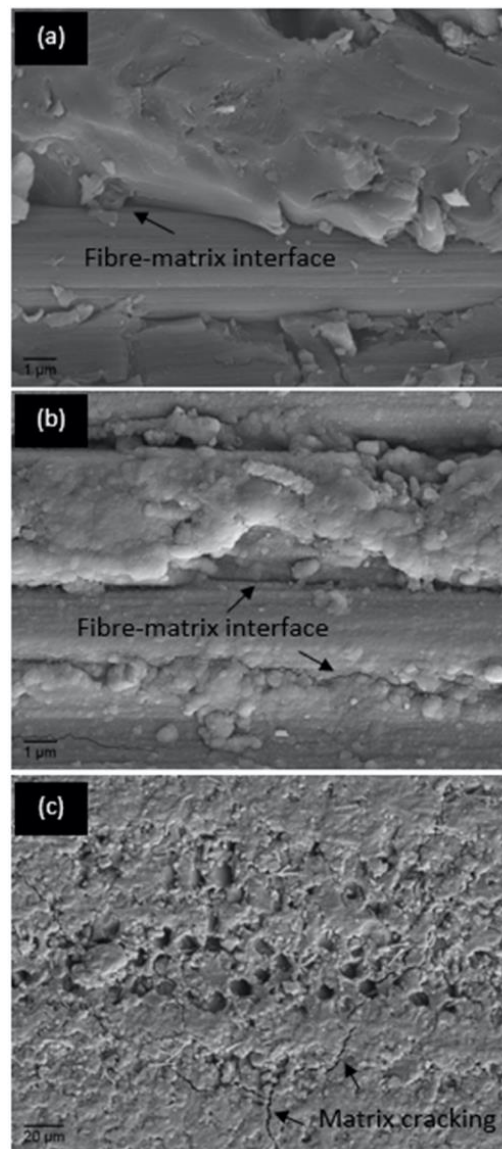


Figure 1: Micrographs of polymer/carbon composites surface: (a) interface of un-aged specimen; (b) interface of aged specimen; (c) matrix cracking in aged specimen [10].

2. Experimental Methods

2.1. Materials

Graphene Nanoplatelets (GNPs) with 5 µm planar size and 15-25 layer thickness, were investigated as reinforcement in this study. Additionally, the effects of surface functionalisation were studied with GNPs undergoing oxygen-based plasma functionalisation, performed through Haydale Ltd's HDPlas® process. XPS analysis determined the unfunctionalised (UFG) and functionalised (FG) GNPs to possess oxygen contents of 2.53 at% and 7.35 at%, respectively. The manufactured nanocomposites combined the respective GNP at 1 wt% filler loading, with low viscosity epoxy resin (Araldite LY1564) and cycloaliphatic polyamine hardener (Aradur 2954) system.

2.2. Sample Fabrication

The respective GNP and epoxy resin were initially combined at 10 wt%, with a SpeedMixer™ DAC 800 at 1950 rpm for 3 minutes. This equipment utilises dual asymmetric centrifugal motion to efficiently homogenise and wet-out the GNPs with epoxy resin. The samples were then high shear mixed using an EXAKT® 80E three-roll-mill, with parameters outlined in Table 1. Increased filler loadings were chosen during this stage to maximise high shear forces present whilst mixing, ensuring good dispersion and the break-down of GNP agglomerates. The mixture was then diluted with epoxy resin to achieve 1 wt% fill loading and homogenised with the SpeedMixer™ for a further 2 minutes at 1950 rpm*, before being placed in a vacuum chamber at -1 bar of pressure for 1 hour to remove trapped air from the system. The hardener was then incorporated at a ratio of 100:35, of epoxy to hardener respectively, and combined with the SpeedMixer™ for a final 2 minutes at 1950 rpm, before being returned into the vacuum chamber for a further 30 minutes. The mixture was slowly poured into an open top aluminium mould with spacer frame, to produce a plaque with dimensions 220mm x 220mm x 4mm. Material was left to cure at room temperature for 18hrs, then post-cured for 1hr at 80°C and 3.5hrs at 140°C. Mechanical test samples were then machined from plaques using CNC milling.

Table 1: Mixing parameters

Pass number	Nip Gap 1 (µm)	Nip Gap 2 (µm)	Roller Speed (rpm)
1-2	45	15	380
3-5	15	5	450

*The procedure from this point onwards was followed for the fabrication of pristine resin samples.

2.3. Moisture Conditioning

The water absorption test set-up is in accordance with ASTM D 5229 [11]; however, a higher water temperature was chosen to accelerate the ageing process. In order to maintain a realistic prediction of long-term water absorption behaviour, it is suggested that the immersion temperature should be at least 20°C lower than the T_g of the matrix [12]. Hydrothermal aging was achieved using Type I purified water in an unstirred digital bath (NE2-28D) of sensitivity ± 0.2 °C and uniformity of ± 0.1 °C set to 90 °C steady state temperature, provided by Clifton. Five of each specimen type were fully immersed for a fixed period of 30 days, exposing all edges to water. Gravimetric measurements were made prior to immersion and at 24hr intervals subsequently. To undertake measurements the samples were removed from the water, wiped free of surface moisture using an absorbent lint-free cloth and placed into sealed bags until reaching a temperature suitable for laboratory handling. Gravimetric measurements of the individual specimens were manually recorded on an analytical balance (Adam Nimbus NBL 623i) with an accuracy of 0.001 g. The samples were then returned into the conditioning chamber, minimising the time out of the sealed bags to 5 min/weighing to avoid moisture losses. The percentage change in weight for the individual specimens on each occasion was calculated using Equation (1):

$$\text{Weight gain, \%} = \frac{W_t - W_b}{W_b} \times 100 \quad (1)$$

Where W_t is the recorded mass of the specimen at the current time t , in g, and W_b is the dry mass of the specimen at baseline time, in g.

2.4. Mechanical Properties

Tensile and flexure testing were carried out to evaluate the mechanical properties of the material in their un-aged and aged conditions. The stress-strain response of the specimens subject to uniform tension and flexure was recorded using an Imetrum Video Strain Gauge (VSG) system that employs Digital Image

Correlation (DIC) principles for precise measurement. Hence, individual specimens were marked within the gauge view for direct strain measurements, detected by the movement of these distinct patterns with respect to their original frame.

The tensile testing was performed on a Shimadzu universal testing machine with 20kN load cell, in accordance with BS EN ISO 527-2:2012. Type 1BA dumbbell-shaped small tensile specimens The tensile specimens (4 mm in thickness, 5 mm in width, and 80 mm in length) were marked at two points within the gauge view (2mm apart over the centre of the gauge length) for percentage strain measurements via the VSG system. Uniaxial tension was achieved by aligning the longitudinal axes of the specimens to the line of action of the loading grip and loaded at a rate of 2 mm/min, until fracture. For the flexural testing, a three-point bend test was carried out in accordance with BS EN ISO 178:2010. The flexural specimens (4 mm in thickness, 10 mm in width, and 95 mm in length) were marked at their mid-span for VSG displacement tracking. Loading was applied using Zwick Roell Z50 load machine, with a loading nose of radius $R_1 = 5 \text{ mm} \pm 0.2 \text{ mm}$ and support rollers of radius $R_2 = 5 \text{ mm} \pm 0.2 \text{ mm}$ (64mm distance between the supports). A 5 N preload was set at a displacement rate of 1 mm/min, after which the cross-head speed was increased to 2 mm/min for the remainder of the test, until failure.

3. Results and Discussions

Figure 2 presents the mass change due to moisture uptake. The mass change observed for graphene enhanced specimens show lower change in values as compared with pristine epoxy resin which indicates that graphene could act as potential barrier to moisture ingress.

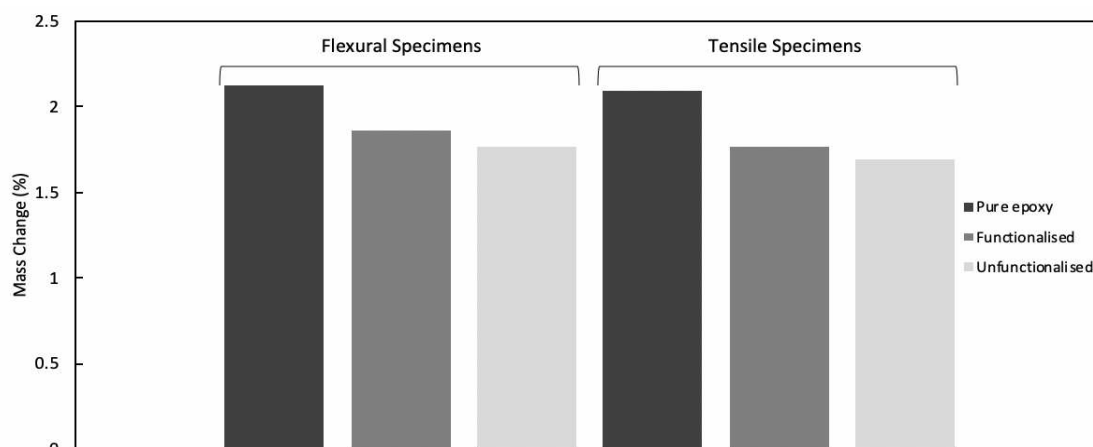


Figure 2: Mass change due to moisture absorption for flexural and tensile specimens prior to mechanical testing.

Figure 3 Figure 4 present the observed mechanical properties for all unaged and aged specimens. Despite the lower mass gain observed (Figure 2), the properties of the nanofilled resins exhibit a larger reduction in properties following water absorption. It is hypothesised that this effect is correlated to moisture degradation at the interfacial graphene/polymer regions leading to potential reduction in stress transfer.

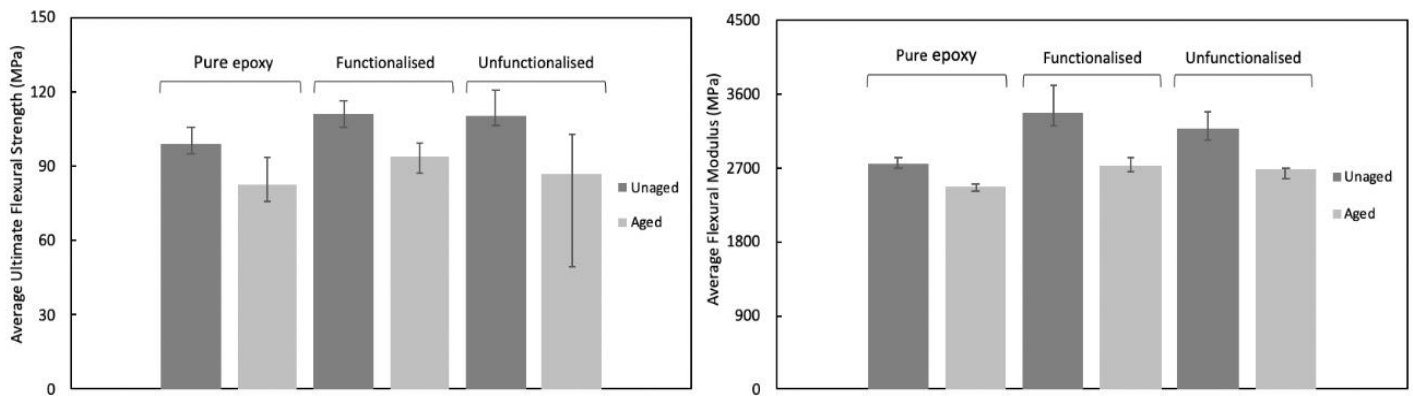


Figure 3: Flexural properties observed for unaged and aged specimens.

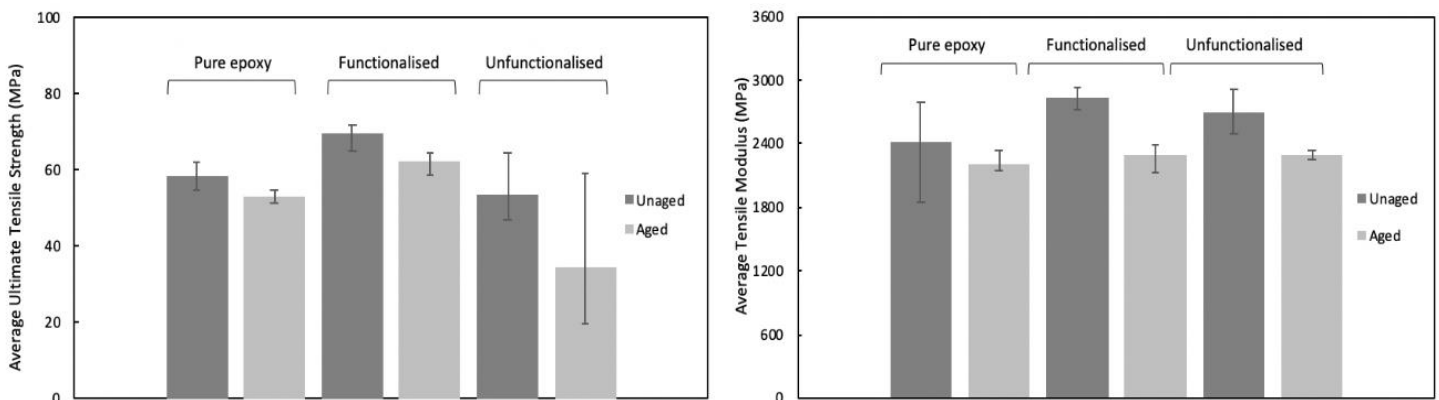


Figure 4: Tensile properties observed for unaged and aged specimens.

4. Conclusions

The study highlights the important role that graphene can play on the mechanical performance of epoxy systems. The performance is however dependent on the environment where the structure is expected to operate. Essential change in behaviour was observed after moisture exposure where specimens with graphene added maintained relatively higher mechanical properties only in the un-aged condition. After aging, higher percentage drops in both strength and modules were observed in those with graphene added specimens. This could further demonstrate the role of the interfacial region [13], and the consequences of aging where less interfacial bonding capability is believed to be present. Further investigations are required particularly with the use of advanced microscopic analysis; for instance, Scanning Electron microscopy (SEM) to gain better understanding of the bonding condition for un-aged and aged specimens.

5. References

- [1] Zafar A, Bertocco F, Schjødt-Thomsen J, Rauhe JC. Investigation of the long term effects of moisture on carbon fibre and epoxy matrix composites. *Compos Sci Technol* 2012;72:656–66.
- [2] Cysne Barbosa AP, Ana AP, S.S. Guerra E, K. Arakaki F, Tosatto M, Maria MC, et al. Accelerated aging effects on carbon fiber/epoxy composites. *Compos Part B Eng* 2017;110:298–306.
- [3] Sethi S, Ray BC. Environmental effects on fibre reinforced polymeric composites: Evolving

- reasons and remarks on interfacial strength and stability. *Adv Colloid Interface Sci* 2015;217:43–67. doi:10.1016/j.cis.2014.12.005.
- [4] Humeau C, Davies P, Jacquemin F. Moisture diffusion under hydrostatic pressure in composites. *Mater Des* 2016;96:90–8. doi:10.1016/j.matdes.2016.02.012.
- [5] Graphene Flagship. Graphene composites enable the aviation industry to gain altitude. 2020.
- [6] Masoumi S, Valipour H. Effects of moisture exposure on the crosslinked epoxy system: An atomistic study. *Model Simul Mater Sci Eng* 2016;24:035011.
- [7] Dao B, Hodgkin J, Krstina J, Mardel J, Tian W. Accelerated aging versus realistic aging in aerospace composite materials. V. The effects of hot/wet aging in a structural epoxy composite. *J Appl Polym Sci* 2010;115:901–10.
- [8] Vasiliev V V, Morozov E V. *Advanced Mechanics of Composite Materials*. vol. 53. 2nd ed. Oxford: Elsevier; 2007.
- [9] Ray BC. Temperature effect during humid ageing on interfaces of glass and carbon fibers reinforced epoxy composites. *J Colloid Interface Sci* 2006;298:111–7. doi:10.1016/j.jcis.2005.12.023.
- [10] Almudaihesh F, Holford K, Pullin R, Eaton M. The influence of water absorption on unidirectional and 2D woven CFRP composites and their mechanical performance. *Compos Part B Eng* 2020;182:107626. doi:10.1016/j.compositesb.2019.107626.
- [11] ASTM International. D5229/D5229M-14e1 Standard Test Method for Moisture Absorption Properties and Equilibrium Conditioning of Polymer Matrix Composite Materials, West Conshohocken, PA: ASTM International; 2014. doi:https://doi.org/10.1520/D5229_D5229M-14E01.
- [12] Bank L, Gentry TR, Barkatt A. Accelerated Test Methods to Determine the Long-Term Behavior of FRP Composite Structures: Environmental Effects. *J Reinf Plast Compos* 1995;14:559–87.
- [13] Park C, Yun GJ. Characterization of interfacial properties of graphene-reinforced polymer nanocomposites by molecular dynamics-shear deformation model. *J Appl Mech Trans ASME* 2018;85:1–10. doi:10.1115/1.4040480.